The kinetics of H2 dissociative chemisorption: The role of transients

Charusita Chakravarty and Horia Metiu

Citation: The Journal of Chemical Physics **102**, 8643 (1995); doi: 10.1063/1.468966
View online: http://dx.doi.org/10.1063/1.468966
View Table of Contents: http://scitation.aip.org/content/aip/journal/jcp/102/21?ver=pdfcov
Published by the AIP Publishing

The kinetics of H_2 dissociative chemisorption: The role of transients

Charusita Chakravarty
Department of Chemistry, University of Cambridge, Lensfield Road, Cambridge, CB2 1EW United Kingdom

Horia Metiu
Department of Chemistry, University of California, Santa Barbara, California 93106-9510

(Received 7 June 1994; accepted 16 February 1995)

The Lee–DePristo model for the dissociative chemisorption of H_2 on Ni(100) has an interesting behavior. The potential energy surface has a minimum corresponding to a molecular, physisorbed state. This minimum is shallow and at 300 K the lifetime of physisorbed H_2 is extremely short. One is then justified in treating the kinetics as a direct dissociation and ignoring physisorption. At 100 K physisorbed H_2 has a long lifetime and one is forced to consider a two-step kinetics: H_2 is first physisorbed and then dissociated. While chemical kinetics describes easily these two limiting cases, it offers little guidance for the intermediate temperature. We show here how the correlation function theory deals with this situation by providing equations which cover all temperature regimes. The theory is general and can be used in all cases when intermediates with shallow wells participate in the reaction mechanism. © *1995 American Institute of Physics.*

I. INTRODUCTION

We focus here on an aspect of dissociative chemisorption[1–6] that arises in a model[5,7–10] of H_2 dissociation on Ni(100), and which is likely to be frequently encountered in other areas of chemical kinetics. The potential energy surface for the H_2/Ni(100) system is such that, at low temperature, dissociation proceeds through two distinct steps: H_2 is first physisorbed and then breaks into chemisorbed H atoms. However, at high temperature the dissociation proceeds directly. Chemical kinetics provides equations for both limiting cases but gives no procedure for dealing with the intermediate temperature.

The key dynamic element that allows us to distinguish the two cases is the mean time spent by the H_2 molecule in the physisorption well. At low temperature this time is substantially longer than the time scale on which molecular motion takes place. Because of this, the transitions of the physisorbed molecule to the gas or to the chemisorbed state are rare events and can be treated as chemical reactions; the phenomenological rate equations provided by chemical kinetics are valid and all reaction dynamics is folded into the rate constants. In the high temperature limit the residence time in the physisorption well is comparable to the time scale of the molecular motion and physisorbed H_2 is no longer a distinct chemical species. The molecule spends a long time either being gaseous or as dissociated into chemisorbed H atoms, but not as a physisorbed molecule. The two long-lived states are chemical species but the physisorbed molecule is not. In this case chemical kinetics equations can describe transitions from chemisorption to gas and back, but have nothing to say about physisorption.

From a microscopic point of view the change in the residence time is a continuous function of temperature, and our description of the kinetics must also change continuously. Phenomenological kinetics, however, shows no such continuity: one has either a one-step or a two-step mechanism and there is nothing in between. To find ''continuous'' kinetic equations we use the correlation function theory (CFT).[12–25] This divides the configuration space into regions located around the minima on the potential energy surface and identifies each minimum with a chemical species. If a minimum traps an equilibrium trajectory for a long time compared to the time scale of the molecular motion, this definition of a chemical species is identical to the one used in conventional chemical kinetics. Otherwise, it is not.

Imagine now that through the agency of some ''external'' force, we drive the populations in various wells out of equilibrium, and then we let them relax. The correlation function theory provides equations describing the rate of this relaxation. If all the wells are sufficiently deep to correspond to chemical species, these equations are identical to those postulated by chemical kinetics. They are however valid even in the situation of interest here, when some of the wells are so shallow that a trajectory lingers in them for an extremely short time.

In those cases when phenomenological chemical kinetics is valid, the CF theory provides equations expressing the rate constants in terms of flux–position correlation functions. In essence these formulas provide the mean flux through the surface surrounding the minimum corresponding to reactants, restricted to those trajectories that will reach the product well and settle in it for a long time. It is because of this long residence time that the rate of the reaction can be described by a time-independent rate constant. If the residence time in the product well is too short, the theory provides an equation containing time-dependent rate constants.

The kinetics of the H_2/Ni(100) system has been studied previously by Truong, Hancock, and Truhlar[26] who used the Lee–DePristo potential[5,7–10] and the variational transition state theory (TST). The TST is a very useful approximation but it does not provide the information of interest to us since it *assumes* that *all* trajectories that cross the dividing surface surrounding the reactant will reach the product region and spend a long time there. TST assumes the validity of the rate equations and cannot help establish how to modify them when the residence time is very short. The CF theory does not have this limitation. The CF theory has an additional

 0021-9606/95/102(21)/8643/13/$6.00

advantage in those cases when systems having more than two wells are studied: It provides expressions for the rate of transition between any given pair of wells, even if they are not adjacent on the potential energy surface. The transition state theory cannot do that: Strictly speaking, it calculates only the rate constant for *getting out* of a well, but not that of getting out *and* reaching a designated well.

The CF approach has been previously used in surface science to study surface diffusion[15,17–25] but has not been applied to dissociative chemisorption. The work presented here is a first step towards such an application. We use in our study the potential energy surface for H_2/Ni(100) constructed and tested by Lee and DePristo.[7–10] *Ab initio* calculations for this system are also available,[11] but they do not provide sufficient points on the potential energy surface to be useful for our purpose. The fact that we use classical mechanics and a rigid lattice limits the accuracy of the rate constant calculation. These approximations are, however, adequate since our purpose is to examine qualitative, generic questions. They need to be removed if a quantitative test of the Lee–DePristo model is intended.

The paper is organized as follows. The geometry of the potential energy surface for H_2/Ni(100) is discussed in Sec. II and the existence of multiple minima is pointed out. The rate equations for the case when the residence time in one of the minima (characterizing one of the chemical species) varies with temperature and becomes too short to allow the use of standard kinetic equations are derived in Sec. III. Much of the mathematics used in the derivation is borrowed from the work of Voter and Doll[15] and Wahnstrom and Metiu.[24,25] The application of the correlation function approach to molecule–surface reactions and the relationship between the calculated and experimental kinetic rate constants is discussed in Sec. IV. The details of the calculation are given in Sec. V. Results of the classical study together with some exploratory estimates of quantum effects are contained in Sec. VI. Section VII is a brief summary.

II. THE MODEL

We use the potential energy surface (PES) constructed by Lee and DePristo.[7] Other PESs have been developed subsequently, and they have the same major topographic features.[8,27] Choosing the Lee–DePristo surface allows us to compare our results to previous rate constant calculations by Truong *et al.*[26]

The atomic positions are measured with respect to a reference frame (X,Y,Z) whose XY plane contains the centers of the atoms in the first surface layer. The Z axis is perpendicular to the surface and points towards the vacuum (Fig. 1). The coordinates of the hydrogen molecule are shown in Fig. 2. The center-of-mass coordinates are $\mathbf{R}=\{X,Y,Z\}$, the hydrogen bond length is r, the angle between the molecular axis and the Z axis is θ, and the azimuthal angle is ϕ.

The dynamics of the reaction is best understood by considering the minimum energy reaction pathway for the two most important coordinates: the distance Z from the center of mass of the H_2 molecule to the surface and the H–H bond length r. We have constructed a ''reduced'' energy surface (RES) by minimizing the potential energy, for given values

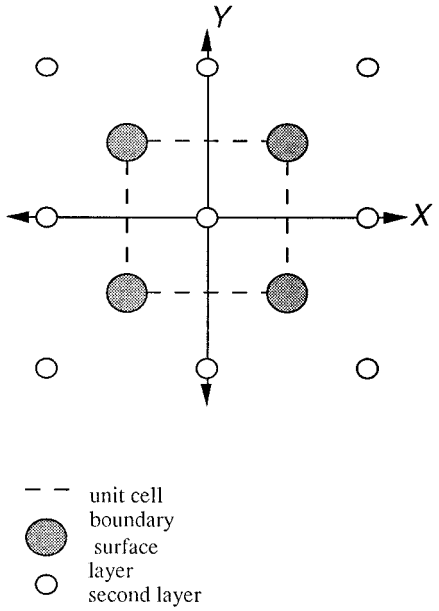

FIG. 1. The position of the fixed coordinate frame (X,Y,Z) with respect to the atoms of the Ni(100) surface.

of Z and r, with respect to the other four molecular coordinates. During this minimization the lattice atoms were held fixed at their equilibrium positions in the solid. The reduced surface is therefore

$$v(Z,r)= \min_{\{\theta,\phi,X,Y\}} V(X,Y,Z,r,\theta,\phi),$$

where V is the potential energy function for the molecule–lattice interaction. A picture of $v(Z,r)$ is shown in Fig. 3.

The zero energy is that of the H_2 molecule at an infinite distance from the metal surface, with r fixed to give the minimum energy. The surface $v(Z,r)$ has a shallow physisorption well (for $1.1<Z<1.5$ Å), with a well depth of 0.13 eV. In this well r is approximately 0.85 Å and the molecule is parallel to the surface. The bond length is slightly greater than the equilibrium value $r=0.75$ Å for the isolated H_2 molecule. A second, very shallow well is observed for

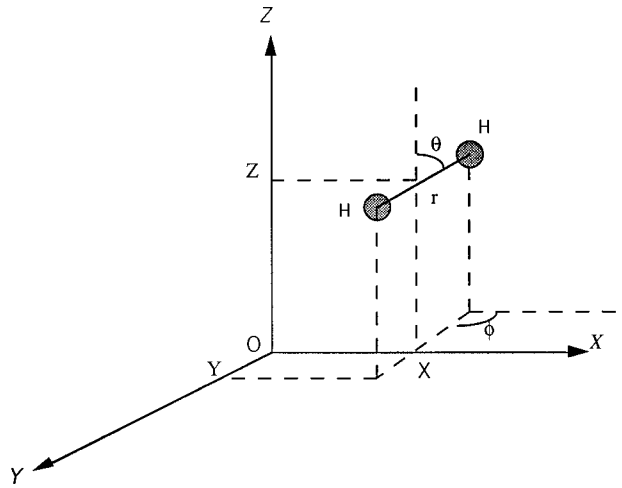

FIG. 2. The coordinates of the H_2 molecule on the Ni(100) surface.

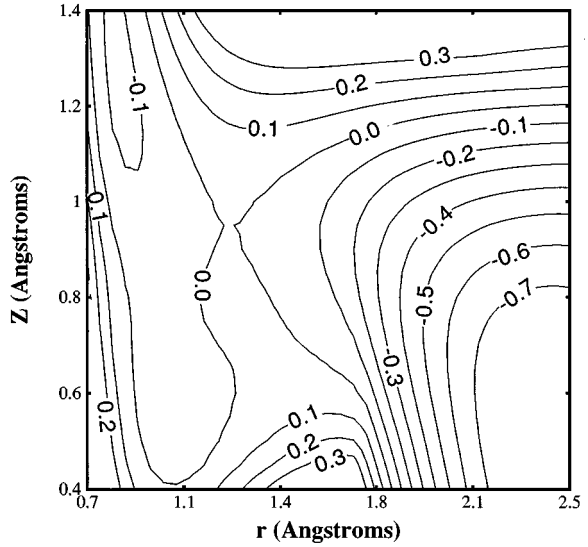

FIG. 3. Contour plot of the reduced energy surface obtained by minimizing the potential energy function at fixed r and Z. The lattice atoms are held rigid during the minimization process and energies are in eV. Contours are plotted at intervals of 0.1 eV.

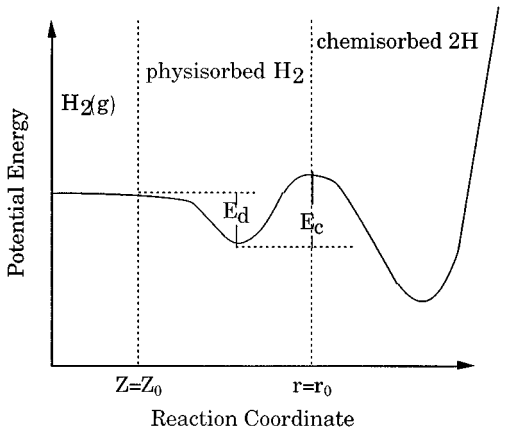

FIG. 4. A schematic representation of the minimum energy pathway on the H_2/Ni(100) potential energy surface. The barriers for chemisorption and desorption are E_c and E_d, respectively.

$Z \cong 0.5$ Å and $r \cong 1.0$ Å. At this minimum the molecule is nearly perpendicular to the surface and is located at the center of the unit cell ($X=0.0$ Å, $Y=0.0$ Å). The RES does not have an energy barrier preventing physisorption.

The chemisorption well has a minimum at $r=2.5$ Å and $Z=0.5$ Å, where the energy is -0.8 eV. This corresponds to two hydrogen atoms adsorbed on adjacent surface cells. The minimum barrier encountered when going from the physisorption well minimum to the chemisorption well (along the reaction path) is 0.13 eV.

The measurements show that the dissociative chemisorption is activated, while our study of the topology of the potential energy surface found a pathway with zero activation energy. There are several ways to interpret this. The simplest is that the PES is incorrect and that there are barriers along the minimum energy path. An alternative is to assume a two-step mechanism: physisorption without activation, followed by an activated reaction from physisorbed H_2 to chemisorbed 2H; the overall process is then activated. Another possibility is that most of the trajectories do not go through the minimum path but through configurations that do encounter a barrier. For example, the (r,Z) plot with H_2 held parallel to the surface ($\theta=90$, $\phi=0$) and X and Y fixed at 0.0 and 1.24 Å, respectively, shows a barrier height for chemisorption of 0.23 eV.[15] These alternatives are not mutually exclusive and they can together explain the existence of an activation energy.

The minimum energy pathway has the structure shown schematically in Fig. 4. The H_2/Ni system is a three-well system with states corresponding to each of the three chemical species: gaseous hydrogen molecule H_2(g), physisorbed hydrogen molecule H_2(a), and chemisorbed hydrogen atoms 2H(a). One important feature of this system is that the barrier preventing the desorption of the physisorbed molecule is very small. As we show later, at low temperatures (e.g., around 100 K) this barrier traps most incident trajectories for a long time, and it makes sense to think that dissociative chemisorption involves three chemical species: gas phase H_2, physisorbed H_2, and chemisorbed hydrogen atoms. The kinetic scheme has the absorption–desorption rate for H_2 and the dissociation step H_2 (physisorbed)$\rightarrow$2H (chemisorbed) and its reverse.

At higher temperatures (300 K or above) the residence time in the physisorbed well is so short that it makes no sense to treat H_2 (physisorbed) as a distinct chemical species. The kinetic scheme therefore should involve a direct reaction H_2(gas)$\rightarrow$2H (chemisorbed) and its reverse. A theory that provides rate equations for all temperatures is discussed in the next section.

III. RATE EQUATIONS FOR SYSTEMS HAVING SHORT-LIVED TRANSIENTS

All molecular theories of chemical kinetics divide the degrees of freedom into a significant group used for defining the chemical species, and the rest. In our example Z and r are such significant variables. Large values of Z together with values of r around the gas phase equilibrium bond length define gaseous H_2; small Z and small r define physisorbed H_2; and small Z together with values of r around the distance between two surface unit cells define chemisorbed 2H. Let us consider a general system for which a reduced set of variables has been defined and the space of these variables has been divided into N regions, each surrounding a minimum in the potential energy surface. These regions do not overlap and are assumed to cover the entire configuration space accessible at the temperatures of interest. Each minimum corresponds to a chemical species.

Let A_α be an operator which confines all integrals over the relevant variables to region α, but does not affect the other variables. The probability that the relevant variables are in the region α when the system is at equilibrium is

$$P_\alpha^{\mathrm{eq}} = \langle A_\alpha \rangle = \mathrm{Tr}\{A_\alpha \exp[-\beta H]\}/\mathrm{Tr}\{\exp[-\beta H]\}. \quad (1)$$

The angular brackets denote, in what follows, the equilibrium thermal average defined by the last equality in Eq. (1).

A system out of equilibrium is described by a time-dependent density matrix $\rho(t)$, and the quantity

$$P_\alpha(t)=\mathrm{Tr}\{A_\alpha\rho(t)\} \tag{2}$$

is the probability that the nuclear configuration of the system is in the region α at time t. The quantity

$$p_\alpha(t)=\mathrm{Tr}\{a_\alpha\rho(t)\}, \tag{3}$$

where

$$a_\alpha=A_\alpha-P_\alpha^{\mathrm{eq}} \tag{4}$$

measures the deviation of the population in the region α from its equilibrium value. At all times we have the conservation conditions

$$\sum_{\alpha=1}^{n} P_\alpha(t)=1, \tag{5}$$

$$\sum_{\alpha=1}^{n} p_\alpha(t)=0. \tag{6}$$

Here, n is the number of distinct chemical species in the system.

Let us now drive the system out of equilibrium and derive equations for the subsequent time-dependent evolution of $p_\alpha(t)$. To do this we use a time-dependent perturbation described by

$$\mathscr{H}=H-\sum_{n=1}^{\infty} f_\alpha \exp[\epsilon t]\theta(t)A_\alpha. \tag{7}$$

Here, H is the unperturbed Hamiltonian of the system, $\theta(t)$ is 1 for $t<0$ and zero for $t>0$, and $\epsilon>0$. The parameters f_α and ϵ are arbitrarily small so that linear response theory is valid, and the disturbance is turned on gently. The physics described by $\mathscr{H}$ is as follows. At $t=-\infty$ the system is in equilibrium. Then, the potential energy surface is distorted infinitesimally slowly so that the system is, at all times, in equilibrium with the modified potential energy surface. At $t=0$ we suddenly go back to the initial potential. This removal of the disturbance leaves the probabilities of finding various chemical species in the system out of equilibrium. After $t=0$ they will relax to the equilibrium values corresponding to the unperturbed Hamiltonian. This procedure is a mathematically convenient way to create nonequilibrium populations and calculate the rate of their relaxation to equilibrium.

We can calculate the nonequilibrium population at time $t>0$ by treating the second term in Eq. (7) as a small perturbation. The result is[28]

$$p_\alpha(t)=\sum_{\alpha=1}^{n} R_{\alpha\lambda}(t)f_\lambda \tag{8}$$

with

$$R_{\alpha\lambda}(t)=\int_0^\beta d\mu\langle a_\alpha(t)a_\lambda(i\mu\hbar)\rangle, \tag{9}$$

$$a_\alpha(t)=\exp[iHt/\hbar]a_\alpha\exp[-iHt/\hbar],$$

and

$$a_\lambda(i\mu\hbar)=\exp[-\mu H]a_\lambda\exp[\mu H]. \tag{10}$$

The time derivative of Eq. (8) gives

$$\frac{\partial p_\alpha(t)}{\partial t}=\sum_{\alpha=1}^{n} C_{\alpha\lambda}(t)f_\lambda, \tag{11}$$

where

$$C_{\alpha\lambda}(t)=\int_0^\beta d\mu\left\langle\frac{\partial a_\alpha(t)}{\partial t}\,a_\lambda(i\mu\hbar)\right\rangle. \tag{12}$$

Equation (8) and the conservation condition [Eq. (6)] lead to

$$0=\sum_{\alpha=1}^{n} p_\alpha(t)=\sum_{\lambda=1}^{n-1} f_\lambda\sum_{\alpha=1}^{n} R_{\alpha\lambda}(t). \tag{13}$$

Since the f_λ are arbitrary, we must have

$$\sum_{\alpha=1}^{n} R_{\alpha\lambda}(t)=0. \tag{14}$$

Using this to eliminate $R_{\alpha n}(t)$ from Eq. (8) gives

$$p_\alpha(t)=\sum_{\alpha=1}^{n-1} R_{\alpha\lambda}(t)(f_\lambda-f_n). \tag{15}$$

The same argument can be used to show that Eq. (11) can be rewritten as

$$\frac{\partial p_\alpha(t)}{\partial t}=\sum_{\alpha=1}^{n-1} C_{\alpha\lambda}(t)(f_\lambda-f_n). \tag{16}$$

The conservation conditions have made one of the variables a_α redundant and we have eliminated the nth one from the kinetic equations.

Solving Eq. (15) for $f_\lambda-f_n$ and using the result in Eq. (16) gives

$$\frac{\partial p_\alpha(t)}{\partial t}=\sum_{\beta=1}^{n-1}\sum_{\gamma=1}^{n-1} C_{\alpha\beta}(t)(R^{-1})_{\beta\gamma}p_\gamma(t)$$

$$\equiv\sum_{\gamma=1}^{n-1}\Gamma_{\alpha\gamma}(t)p_\gamma(t), \tag{17}$$

where R^{-1} is the inverse of the matrix R.

This set of linear equations is valid regardless of how the partitioning of the space was made. We could, if we wish, use them to study how the probability that the bond length is in a certain range relaxes to its equilibrium value after it was driven somehow out of equilibrium. If each region surrounds a sufficiently deep minimum on the potential energy surface, the probability of being in region α is the probability that the chemical species α is present in the system. In such cases,

Eqs. (17) must be identical to those of chemical kinetics. In particular the "rate constants" $\Gamma_{\alpha\gamma}(t)$ in Eq. (17) must be time dependent.

To show why this is indeed the case we have to analyse how $R_{\alpha\beta}(t)$ and $C_{\alpha\beta}(t)$ depend on time. Consider the response function $C_{\alpha\lambda}(t)$ which can be written as

$$C_{\alpha\lambda}(t)=\int_0^\beta d\mu\left\langle\left(\frac{\partial a_\alpha(t)}{\partial t}\right)a_\lambda(i\mu\hbar)\right\rangle$$

$$=\int_0^\beta d\mu\langle(i[H,a_\alpha(t)]/\hbar)a_\lambda(i\mu\hbar)\rangle$$

$$=\int_0^\beta d\mu\langle(i[H,a_\alpha(0)]/\hbar)a_\lambda(i\mu\hbar-t)\rangle. \tag{18}$$

Using the definition of $a_\alpha(0)$ we calculate that

$$i[H,a_\alpha(0)]/\hbar=[p^2/2m,a_\alpha]$$

$$=(i\hbar/2m)\left\{\left(\frac{\partial a_\alpha}{\partial x}\right)p-p\left(\frac{\partial a_\alpha}{\partial x}\right)\right\}=F_\alpha. \tag{19}$$

Here, a_α is the characteristic function defining the region α and $\partial a_\alpha/\partial x$ is a δ function which confines the coordinates to the border of the region α. Since p/m is a velocity operator, the commutator in Eq. (18) gives to the flux F_α through the border of the region α. Therefore, the quantities $R_{\alpha\lambda}(t)$ and $C_{\alpha\lambda}(t)$ correspond to position–position and flux–position operators, respectively.

The physical interpretation of these quantities allows us[13(a)] to establish the time scale on which they decay. This is best seen by discussing how these quantities are computed in the classical limit. To obtain $R_{\alpha\lambda}(t)$ we must use a Monte Carlo procedure to place the system in the region α with the appropriate equilibrium velocities and positions. Then we must let the system evolve and follow it until it settles in the region λ. Since we assume that the two regions are separated by a large energy barrier, this event takes a very long time on the scale of the molecular motion. In fact this time is of the order of the inverse of the rate constant for the reaction from α to λ. The flux–position function $C_{\alpha\lambda}(t)$ has an entirely different character. When $C_{\alpha\lambda}(t)$ is calculated the reaction coordinate of the system must start (because of the presence of the flux operator) on the dividing surface surrounding region α. It is placed there by an equilibrium Monte Carlo procedure and then it is let go and is followed until it settles in region λ. If α and λ are adjacent in space, this happens in a few tens of femtosecond.[19] Thus $C_{\alpha\lambda}(t)$ becomes a constant very rapidly (in 100 fs or less) and $R_{\alpha\lambda}(t)$ evolves very slowly. Since, to obtain the rate constant, we need only follow the system until $C_{\alpha\lambda}(t)$ becomes constant, we can take $R_{\alpha\lambda}(t=0)$ in Eqs. (12) through (16). This means that except for the first 100 fs after we started our relaxation experiment, $\Gamma_{\alpha\gamma}(t)$ is independent of t. After this initial transient, Eq. (16) has the same form as the phenomenological rate equations for a multisite system.

This result relies on the assumption that the barriers between the regions exceed kT by a safe margin; This ensures that the time scale on which $R_{\alpha\gamma}(t)$ and $C_{\alpha\gamma}(t)$ evolve are very different. As kT becomes comparable to one of the barriers surrounding a site (say α), the quantities $R_{\alpha\gamma}(t)$ can evolve as fast as $C_{\alpha\gamma}(t)$. This happens because a particle in equilibrium at α will not live there for long; the high temperature has turned the species α into a transient. In this case we cannot use $R_{\alpha\gamma}(t)\cong R_{\alpha\gamma}(0)$, but must explicitly include the time evolution of this quantity.

In the case considered here only the H_2 well is shallow enough to become a transient at higher temperature. In this case the problem of what the phenomenological rate equations are and how the shallow well affects them is simplified by the conservation equation. This means that we are free to ignore one population in the rate equations and we can chose the transient population for that. Thus if we label by 1 the gas phase H_2, by 3 the transient region, and by 2 the chemisorbed 2H, we can write Eq. (16) in terms of $p_1(t)$ and $p_2(t)$ only. For example,

$$\frac{\partial p_2(t)}{\partial t}=(C_{21}(R^{-1})_{11}+C_{22}(R^{-1})_{21})p_1(t)$$

$$+(C_{21}(R^{-1})_{12}+C_{22}(R^{-1})_{22})p_2(t).$$

Thus we have only two species in the equations, H_2 in gas and 2H on the surface. The question is: does the presence of the H_2 well affect these equations? If the temperature is very low the effect on R_{12} is that many trajectories that start in 1 do not make it to 2; they get stuck in the intermediate region 3 (adsorbed H_2). Thus R_{12} is diminished by the presence of the well. As the temperature is increased R_{12} will grow. However, since the barrier along the reaction path from 1 to 2 is large R_{12} varies always slowly with time.

When C_{12} is evaluated a particle starts on the border between 1 and 3 and it is followed until it reaches 2. At low T, the particle will either get stuck in 3 or will reach 2. If it gets stuck in 3 it does not contribute to C_{12} and therefore it does not affect the magnitude or the time dependence of C_{12}. A few trajectories that reach 2 directly (without being trapped in 3) will get there very rapidly. Examples of such calculations can be found in Refs. 19, 24, and 25, where the role of multiple jumps in diffusion was studied. Thus at low T, $C_{12}(t)$ varies very rapidly with time.

If the temperature is higher, trajectories starting on the dividing surface surrounding 1 will be delayed but not trapped in 3. For this reason $C_{12}(t)$ will take a long time to reach the "plateau region,"[13(a)] which is the time when the phenomenological theory is valid.

At even higher temperatures the trajectory has enough energy to pass through 3 without considerable delay and the system has effectively only two wells. The concentration in 3 is practically zero and a two-well theory and the corresponding phenomenology can be used. It is the intermediate temperature region that is troublesome. There both $R_{12}(t)$ and $C_{12}(t)$ vary slowly with time and the time scale separation needed for Γ to become constant does not take place. The rate equations have time-dependent rate constants.

For later reference we note that in the temperature regime in which the phenomenological kinetic equations are valid, the rate constant for a reaction consisting of a transfer from region α to region β is given by[15,24,25]

$$k_{\alpha\beta}=\lim_{t\to\infty} C_{\alpha\beta}(t)/Q_\alpha . \tag{20}$$

The infinity is the short time in which $C_{\alpha\beta}(t)$ becomes a constant. The quantity

$$Q_\alpha=\mathrm{Tr}\{A_\alpha \exp[-\beta H]\} \tag{21}$$

is the partition function of the species α.

IV. APPLICATION TO H_2 CHEMISORPTION: THE CONNECTION TO THE EXPERIMENTAL RATE CONSTANTS

In this section we apply the correlation function theory (see Sec. III) to the case of H_2 chemisorption. To do this, we review briefly the empirical analysis. This allows us to define the notation and clarify what is being computed. A minor complication appears because the correlation function theory works with the probability that the nuclei are located in a certain region of the configuration space, while the empirical equations use surface coverage and concentrations.

A. The experimental rate equations

At low temperature the physisorbed H_2 must be treated as a distinct chemical species. The reactions are

$$\mathrm{H_2(g)}+S\underset{k_d}{\overset{k_p}{\rightleftarrows}}\mathrm{H_2(a)}, \tag{22}$$

$$\mathrm{H_2(a)}\underset{k_r}{\overset{k_c}{\rightleftarrows}}2\mathrm{HS}. \tag{23}$$

Here, S is a vacant surface site, k_p is the physisorption rate coefficient, k_d is the rate constant for the desorption of physisorbed H_2, k_c is the rate constant for the dissociation of a physisorbed molecule $[H_2(a)]$, and k_r is the rate constant for the recombination of two H atoms adsorbed on two adjacent S sites. We neglect here the role of surface diffusion; this is customary although not always justified. Furthermore, we assume that the measurements are made at a low coverage and we need not worry about the coverage dependence of the rate constants and the fact that the number of surface sites available for adsorption varies with time. The rate equations corresponding to the above mechanism are[1]

$$A^{-1}\frac{dN_g}{dt}=-k_p[\mathrm{H_2}]_\mathrm{g}[S]+k_d[\mathrm{H_2}]_\mathrm{a}, \tag{24}$$

$$A^{-1}\frac{dN_p}{dt}=-k_d[\mathrm{H_2}]_\mathrm{a}+k_p[\mathrm{H_2}]_\mathrm{g}[S]-k_c[\mathrm{H_2}]_\mathrm{a}[S]^2+k_r[\mathrm{HS}]^2, \tag{25}$$

$$A^{-1}\frac{dN_c}{dt}=k_c[\mathrm{H_2}]_\mathrm{a}[S]^2-k_r[\mathrm{HS}]^2, \tag{26}$$

where N_g, N_p, and $2N_c$ are the number of gas-phase, physisorbed hydrogen molecules, and chemisorbed hydrogen atoms, respectively. The concentrations $[H_2]_g$, $[S]$, $[H_2]_a$, and $[HS]$ have units of molecule/cm^3, site/cm^2, molecule/cm^2, and atom/cm^2, respectively. A is the area under observation.

It is customary to assume that the concentration of the intermediate physisorbed H_2 reaches a steady state. In this case the overall rate constant for H_2 chemisorption is $k=k_pk_c/(k_d+k_c)$. The stationarity of $[H_2]_a$ makes the reaction appear to be a first-order direct dissociation. However, it is not. The existence of a two-step mechanism affects the magnitude and the temperature dependence of the measured rate constant k. For example, in general one expects that k will not have an Arrhenius temperature dependence. Unfortunately, it is often the case that k has accidentally an Arrhenius temperature dependence, especially when the temperature range of the measurements is small. Unfortunately, this prevents us from realizing that the measured rate is not one-step, and also provides us with an activation energy that may have nothing to do with the barrier to chemisorption.

At high temperature (when the barrier defining the physisorbed H_2 is not much larger than kT) the dissociation reaction is direct

$$\mathrm{H_2(g)}+2S\underset{k_{rd}}{\overset{k_{cd}}{\rightleftarrows}}2\mathrm{HS}. \tag{27}$$

The corresponding rate equation is

$$A^{-1}\frac{dN_g}{dt}=-k_{cd}[\mathrm{H_2}]_\mathrm{g}+k_{rd}[\mathrm{HS}]^2. \tag{28}$$

B. The correlation function theory formulas for the rate constants

To use the correlation function theory we must specify the regions in the configuration space defining the chemical species involved in the reaction. The center of mass of H_2 has the coordinates X,Y,Z (see Fig. 2). The gas molecules are defined by the condition $Z>Z_0$. Here, Z_0 defines a plane parallel to the surface which is far enough from the physisorption well. Ideally, the plane should be located on the top of the barrier preventing the H_2 molecule from desorbing. If there is no such barrier a good choice would be to place the plane at a distance Z_0 where H_2 stops interacting with the surface. If one uses the transition state approximation, the choice of Z_0 at the top of the barrier is very important; any other choice leads to errors. If the correlation function theory is applied numerically exactly, then the choice of Z_0 is not essential; a poor, but reasonable, value for Z_0 leads to diminished computational efficiency but not to erroneous results. We take advantage of the translational symmetry along the surface and confine the variables X and Y within the surface unit cell defined in Fig. 1. Finally, the bond length needs to be confined, in principle, to values smaller than those at which H_2 breaks up. However, since the bond strength is very large compared to the values of kT of interest here, the Boltzmann factors in the equations will prevent the variable r from reaching these values anyway, so the restriction is not necessary. We introduce the function $A_g(X,Y,Z,r)$ which is one when the constraints described above are satisfied and zero otherwise. The probability that the H_2 molecule is in the gas phase at time t is then given by

$$P_g(t)=\mathrm{Tr}\{A_g(X,Y,Z)\rho(t)\}, \tag{29}$$

where $\rho(t)$ is the density matrix of the system at time t. The total number of particles in gas at time t is $N_g(t)=NP_g(t)$, where N is the total number of H_2 molecules introduced initially in the system.

The region defining the physisorbed molecule H_2(a) is $Z<Z_0$, X, Y within the surface unit cell, and the bond length $r<r_0$. Here, r_0 is the location of the energy barrier along the reaction path for the dissociation of the physisorbed H_2 into two chemisorbed atoms. $A_p(X,Y,Z,r)$ is one if these conditions are satisfied and zero otherwise. The probability $P_p(t)$ of finding a physisorbed molecule in the system at time t is $P_p(t)=\mathrm{Tr}\{A_p(X,Y,Z,r)\rho(t)\}$, and $N_p(t)=NP_p(t)$. Finally, chemisorption is defined by $Z<Z_0$ and $r>r_0$ and the corresponding function is $A_c(X,Y,Z,r)$. The two hydrogen atoms can be located anywhere on the surface as long as their bond distance is large enough to qualify them as being dissociated. Since the H atoms have well-defined preferences for specific surface sites it is not difficult to decide whether the dissociation has occurred or not.

We consider first the general case when we need to take into account three regions of the configuration space, gas phase H_2, physisorbed H_2, and dissociated chemisorbed H atoms. If the physisorbed molecule is an intermediate (i.e., has a sufficiently long life time to be considered a chemical species), the correlation function theory provides us with the rate equation

$$\frac{dP_g(t)}{dt}=-k_{gp}P_g(t)+k_{pg}P_p(t), \tag{30}$$

$$k_{gp}=\lim_{t\to\infty}(Q_p^{\#}/Q_g)C_{gp}(t), \tag{31}$$

$$Q_p^{\#}C_{gp}(t)=\int d\mathbf{R}\,d\mathbf{P}\,d\mathbf{r}\,d\mathbf{p}\;v_Z(0)\delta[Z(0)-Z_0]\times A_p(X,Y,Z(t),r(t))\exp[-\beta H], \tag{32}$$

$$Q_p^{\#}=\int d\mathbf{P}\,d\mathbf{R}\,d\mathbf{p}\,d\mathbf{r}\;\delta(Z-Z_0)\Delta(X,Y)\exp[-\beta H], \tag{33}$$

$$Q_g=\int d\mathbf{P}\,d\mathbf{R}\,d\mathbf{p}\,d\mathbf{r}\,A_g\,\exp[-\beta H_g]. \tag{34}$$

Here, $\Delta(X,Y)$ is one if X and Y are within the surface unit cell and zero otherwise. These equations are obtained by taking the classical limit in Eqs. (20) and (21). The ''transition state'' partition function $Q_p^{\#}$ is introduced in the equations so that we can write the correlation function $C_{gp}(t)$ in a form amenable to integration by the Monte Carlo method. If we regard, in the Monte Carlo evaluation, $C_{gp}(t)$ as the average of $v_Z(0)A_p(X,Y,Z(t),r(t))$ with the probability $\delta[Z(0)-Z_0]\Delta(X,Y)\exp[-\beta H]$, then the MC procedure will give us the integral we seek divided by the integral over the probability; the latter is $Q_p^{\#}$. The flux–position function $C_{gp}(t)$ correlates the flux crossing the surface dividing the gas from the physisorption region at time zero with the probability of being in the physisorption region at time t. The integral over X and Y in C_{gp}, C_{pg}, Q_p, Q_g, and $Q_p^{\#}$ is over the surface unit cell, and the momentum integrals are over all momenta (not just those values for which the molecule goes from gas to the physisorbed state). The limit to infinite time is actually to the time when $C_{gp}(t)$ becomes constant. This is of the order of a few hundred femtoseconds.[13(a),19] If the system is not trapped in the physisorption well, the function $C_p(t)$ will not reach a plateau value but will grow and then decay to zero on a ''molecular time scale.''

If molecular adsorption and molecular desorption were the only rates, then we could calculate the desorption rate by using detailed balance: the ratio of the rate constants equals the equilibrium constant. However, if three species (and four rates) are needed for describing the system the detailed balance condition is more complex; there are two equilibrium constants and their connection with the rate constants is a little more complicated.

In the case when physisorbed H_2 is a chemical species we can calculate the desorption rate constant from

$$k_{pg}=\lim_{t\to\infty}(Q_p^{\#}/Q_p)C_{pg}(t), \tag{35}$$

$$Q_p^{\#}C_{pg}(t)=\int d\mathbf{R}\,d\mathbf{P}\,d\mathbf{r}\,d\mathbf{p}\;v_Z(0)\delta[Z(0)-Z_0]\times A_g(X,Y,Z(t),r(t))\exp[-\beta H]. \tag{36}$$

Note that Eq. (36) can be obtained from Eq. (32) through the replacements $Q_g\to Q_p$ and $A_p\to A_g$. If only two species were present then $A_p=1-A_g$, $C_{pg}(t)=C_{gp}(t)$ and $k_{pg}/k_{gp}=Q_p/Q_g$, which is the detailed balance equation. However, if three species are present then $A_p=1-A_g-A_c$ and the detailed balance involves k_{pc} also.

If we apply the theory to the direct dissociation reaction [Eq. (27)] we obtain

$$\frac{dP_c(t)}{dt}=-k_{cp}P_c(t)+k_{pc}P_p(t) \tag{37}$$

with

$$k_{pc}=\lim_{t\to\infty}(Q_c^{\#}/Q_p)4C_{pc}(t), \tag{38}$$

$$Q_c^{\#}C_{pc}(t)=\int d\mathbf{R}\,d\mathbf{P}\,d\mathbf{r}\,d\mathbf{p}\;v_Z(0)\delta[Z(0)-Z_0]\times\Delta(X,Y)A_c(Z(t))\exp[-\beta H]. \tag{39}$$

The reverse rate k_{cp} is obtained by replacing $A_c\to A_p$ and $Q_p\to Q_c$. The definition of Q_c is similar to that of Q_g and Q_p. The comments made above Eq. (37) also apply here. The factor of 4 appears because there are four identical pathways for H_2 dissociation, in which one atom remains in the surface cell in which the H_2 molecule approaches the surface and the other is in one of the four equivalent neighboring cells. The correlation function contains only one of the four dividing surfaces and this is why it is multiplied by four.

The rate constants provided by the correlation function theory differ from the rates k_p and k_d which appear in the phenomenological equations because the units of concentration are different. However, a connection can be made by comparing Eq. (30) to the empirical equation (22). To do this we rewrite Eq. (30) in the form

$$A^{-1}\frac{dN_g}{dt}=-k_{gp}(V/A)(N_g/V)+k_{pg}(N_p/A). \tag{40}$$

We have used the fact that $N_g=NP_g$ and $N_p=NP_p$. Since $N_g/V=[H_2]_g$ and $N_p/A=[H_2]_a$ we can compare Eq. (40) with Eq. (24) to obtain

$$k_{gp}V/A=k_pS_0. \tag{41}$$

Here, S_0 is the number of absorption sites per unit area.

It may seem rather strange that the connection between the measured rate k_p and the calculated rate k_{pg} involves the length $L=(V/A)$ of the box in which the gas is located. This is not, however, entirely unexpected. The absorption rate, for example, depends on the incident flux which is a function of pressure, which in turn depends on the volume of the gas. If the area of the box is fixed by the surface of the sample, then the rate given by the correlation function theory depends on the length of the box. The experimental rate constant does not, since from Eqs. (41) and (31) we obtain

$$k_p=k_{gp}L/S_0=\lim_{t\to\infty}(Q_p^{\#}L/S_0Q_g)C_{gp}(t) \tag{42}$$

and Q_g is proportional to L.

The rate constant k_{pg} is the same as the experimentally measured desorption rate k_d, the dissociation rate k_c is the same as k_{pc}, and the recombination rate constant k_r is the same as k_{cp}.

If the temperature is so high that the dissociation is direct then the definition of the chemical species in the correlation function theory must be adjusted accordingly. The ''gas phase'' geometry is now defined by A_g+A_p and the chemisorbed state by A_c. The dividing surface between the physisorbed and the chemisorbed species separates now the chemisorption region from the gas. A trajectory that crosses this surface from the chemisorption region to the physisorbed one is most likely to move to the gas phase on a very short (molecular) time scale. The definitions of the rate constants are then modified accordingly. The connection to the empirical rate is easily made along the lines discussed above.

At intermediate temperature we have a situation which is ill defined, from the point of view of the empirical kinetic equations. These allow no continuous transition between the low and the high temperature regimes. The kinetic equations provided by the correlation function theory are valid in all regimes. However, as the temperature is increased the correlation functions C_{gp} and C_{cp} no longer have a plateau but decay to zero on a fast time scale. This time scale becomes shorter as the temperature is raised. The corresponding rate constants are, in this regime, time dependent. At high temperature their contribution to the system of kinetic equations becomes negligible.

V. SOME COMPUTATIONAL DETAILS

We need to calculate two kinds of quantities: the flux–position correlation functions and the ratios between the partition function of the transition state and that of reactants. Both are calculated by the Monte Carlo method.

To obtain correlation functions an MC program[29,30] is used[19] to generate the coordinates of the system at equilibrium, with the reaction coordinate constrained to be located on the appropriate dividing surface. The momenta are generated from a Maxwell distribution. A Verlet algorithm with a stepsize of 0.2 fs finds how the two hydrogen atoms move when they are no longer constrained to the dividing surface. We use 5000 initial configurations to calculate the appropriate MC averages. Throughout all of this, the lattice atoms are held at their equilibrium positions.

To calculate the flux–position correlation functions and the partition functions of the transition states we need to specify the positions of the dividing surfaces. For calculations having to do with the adsorption and the desorption of physisorbed H_2 we use X, Y confined to the surface unit cell $(-1.24<X,Y<1.24)$, the H_2 bond length $r=1.25$, and $Z=Z_0$ with $Z_0=2.0$, 2.5, and 3.0 Å. The use of three different values for Z_0 allows us to understand absorption dynamics in more detail. To calculate the rate of physisorbed H_2 dissociation we use $r=1.25$ Å with no other constraints. In particular, the bonding of the H atoms to the surface is so strong that we do not need to confine the well in the Z direction; the Monte Carlo procedure will avoid large Z regions automatically.

There are good reasons to believe that one cannot define rate constants if the lattice atoms are not allowed to move and to provide thus a dissipative ''heat bath.'' The system reacts because occasionally the system manages to reach the dividing surface and cross into the well describing the products. When located on the dividing surface the system has an unusually large amount of energy in the reaction coordinate. The role of the heat bath is to remove this energy and localize the system in the product region. When this happens the flux–position correlation function becomes time independent, and this constant value is used to calculate the rate constant. Without this constancy the phenomenological rate equations and the concept of rate constant need to be modified.

The key element here is not the existence of a heat bath but the presence of a mechanism which *removes energy from the reaction coordinate*. Such a mechanism exist even if the lattice motion is frozen, making the heat bath inactive, because the reaction coordinate is coupled to the other degrees of freedom of the reacting molecule. A instructive example of such ''self-trapping'' mechanism has been provided in Refs. 19, 20, 24, and 25 for the case of the hydrogen atom diffusion on a metal surface. In those calculations, an atom that crosses the dividing surface between two energy wells, which define two absorption sites, is trapped in the final well because its energy is rapidly transferred from the reaction coordinate (motion parallel to the surface) to the motion perpendicular to the surface. The energy left in the reaction coordinate is insufficient to get the atom out of the final well. The details of this self-trapping process and its dependence on the atom–surface interaction has been studied in detail by Zhang *et al.*[31] This mechanism will not trap the particle for a very long time since the energy will return, sooner or later, back into the reaction coordinate; the simpler the system, the shorter the time of return. Nevertheless, self-trapping is very important because it is, in many systems, much more rapid than trapping by energy exchange with the heat bath. In the

TABLE I. The classical partition function Q_g/L for the gas phase H_2 molecule, the physisorbed intermediate Q_p, and the transition state $Q_p^{\#}$ for the physisorption process. The units are eV, Å, and femtosecond. The error bars for the calculated values of Q_g/L and $Q_p^{\#}$ are less than 1%. The error bars for Q_p are of the order of 10%.

	Temperature=100 K			Temperature=300 K			Temperature=500 K		
Z_0 (Å)	Q_g/L	$Q_p^{\#}$	Q_p	Q_g/L	$Q_p^{\#}$	Q_p	Q_g/L	$Q_p^{\#}$	Q_p
2.0	1.68	2.54	2.56 (3)	2.92	1.78	5.21	3.78	2.42	3.2
2.5		0.94			2.26	6.91		3.29	5.6
3.0		1.33			2.70	8.85		3.69	7.2

example of H diffusion[19,20,24,25] the mass disparity between the hydrogen atom and the metallic surface is so large that energy transfer to phonons is very slow. Self-trapping occurs in about 100 fs which is much faster than the time it takes to excite phonons and possibly electron hole pairs. If self-trapping is the fastest trapping mechanism, then the role of the energy transfer to the heat bath is to make self-trapping "permanent" (until the reverse reaction takes place). Thus one may assume that a self-trapped molecule becomes permanently trapped because of the bath. The certainty that this will happen allows us to use a rigid lattice in the simulation, without making significant qualitative errors.

As seen from Eq. (42) we need to calculate Q_g/L. If the dividing surface is located at a position where the molecule no longer interacts with the surface then Q_g is proportional to L and the experimental rate coefficient k_p will not depend on L. We calculate Q_g classically and confine the coordinates X and Y to the surface unit cell (Fig. 1). The interaction energy between the two hydrogens is $D\{1-\exp[-\alpha(r-r_e)]\}^2$ with $D=4.747$ eV, $\alpha=1.9417$ Å^{-1}, and $r_e=0.7416$ Å.[32] The unit cell parameter for the square surface lattice of Ni(100) is 2.48 Å. Values of Q_g/L at 100, 300, and 500 K are listed in Table I.

To evaluate the partition function $Q_p^{\#}$ for the H_2 molecule confined to the dividing surface between the gas phase and the physisorption region we use the equation

$$Q_p^{\#}/Q_0=\frac{\int d\tau\ \delta(Z-Z_0)\Delta(X,Y)e^{-\beta(H-H_0)}e^{-\beta H_0}}{\int d\tau\ \delta(Z-Z_0)\Delta(X,Y)e^{-\beta H_0}}. \quad (43)$$

The integration $d\tau$ is over the six coordinates describing the configuration of the molecule. Since

$$Q_0=\int d\tau\ \delta(Z-Z_0)\Delta(X,Y)e^{-\beta H_0}. \quad (44)$$

Equation (43) is identical to the definition of $Q_p^{\#}$. The right hand side of Eq. (43) can be calculated by the Monte Carlo procedure with the sampling function $\exp[-\beta H_0]$. The Hamiltonian H_0 is chosen so that Q_0 given by Eq. (44) can be calculated analytically or by a simple numerical integration. We use for H_0 a Morse potential with the same parameters as the ones used for the gas phase molecule but with α replaced with 0.7α. The integration over the bond distance, needed for computing Q_0, is done numerically. The values of Q_p are shown in Table I, for several choices of Z_0.

The partition function Q_p, of the physisorbed H_2, was calculated with a different procedure[29,33] since we were unable to find a simple sampling function for which the convergence of the procedure described above was satisfactory. We make use of the equation

$$\ln\{Q_p/Q_0\}=\int_0^1 d\lambda\langle V-V_0\rangle_\lambda, \quad (45)$$

where

$$\langle V-V_0\rangle_\lambda=\int d\tau\ A_p[V-V_0]e^{-\beta V_\lambda}\ \Big/\ \int d\tau\ A_p e^{-\beta V_\lambda} \quad (46)$$

and

$$V_\lambda=V_0+\lambda(V-V_0). \quad (47)$$

The function A_p was defined in Sec. IV and its role is to confine the integration (over the six variables characterizing the H_2 molecule) to the physisorption region ($Z<Z_0$, $r<r_0$, and X, Y within the surface unit cell). The reference potential (used for V_0 in the above equations) is

$$V_{0p}=k(Z-Z_e)^2/2+D\{1-\exp[-\alpha(r-r_e)]\}+V_e \quad (48)$$

with $k=0.8$ eV/Å^2, $Z_e=1.3$ Å, $V_e=-0.125$ eV, $\alpha=1.36$ Å^{-1}, $r_e=0.82$ Å, and $D=4.74$ eV. The computed partition functions and free energies of physisorbed H_2 are presented in Table I.

The dividing surface for dissociation, separating reactants (physisorbed H_2) and products (dissociated H_2), is de-

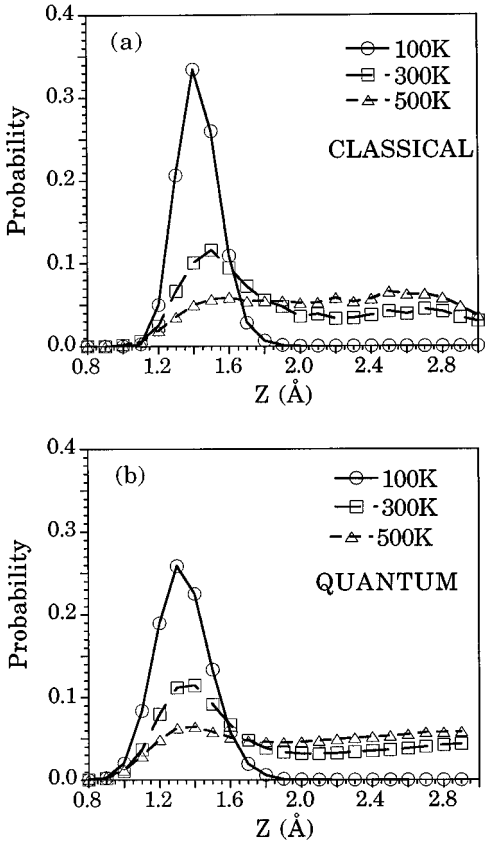

FIG. 5. Classical and quantum canonical probability distributions along the Z coordinate at 100, 300, and 500 K.

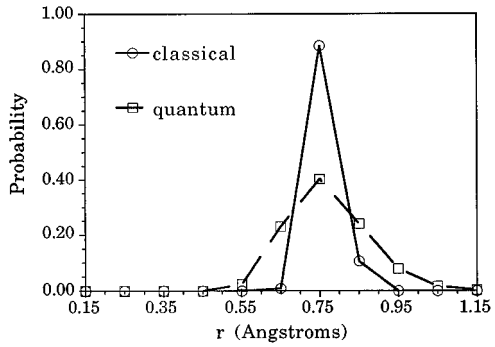

FIG. 6. Classical and quantum canonical probability distributions along the r coordinate at 100 K.

fined by $r=1.25$ Å. The partition function $Q_c^{\#}$ was computed by the integration method provided by Eqs. (45) through (47). The reference potential is

$$V_{0c}(X,Y,\theta)=0.6R^2+0.4\{[\cos(\theta)+0.95]^2+[\cos(\theta)-0.95]^2\} \quad Z<0.7 \text{ Å}, \tag{49}$$

$$V_{0c}(X,Y,\theta)=0.3(R-0.45)^2+0.4\{[\cos(\theta)+0.75]^2+[\cos(\theta)-0.75]^2\} \quad Z>0.7 \text{ Å}. \tag{50}$$

Here $R=(X^2+Y^2)^{1/2}$. The integrals over Z and ϕ were calculated by uniform sampling in the ranges 0.4 Å$<Z<$1.5 Å and $0<\phi<2\pi$.

To explore the magnitude of the quantum effects we have also calculated the quantum mechanical canonical probability distribution along various coordinates for particles in the region of the physisorption minimum. To generate the canonical probability distribution we used a Fourier path quantum Monte Carlo procedure.[34] For each hydrogen atom, at temperatures of 100, 300, and 500 K, the number of Fourier coefficients employed was 32, 16, and 16, respectively.

VI. RESULTS

One way of deciding whether physisorbed H_2 is an intermediate species in chemical kinetics is to look at the probability that Z has a specified value when the system is in equilibrium [Fig. 5(a)]. At 100 K both the classical [Fig. 5(a)] and the quantum [Fig. 5(b)] distributions are peaked around the minimum in the desorption well ($Z=1.3$ Å) and the probability of observing $Z>2.0$ Å is virtually zero. This means that reaching the dividing surface separating the physisorption region from the gas phase one is a rare event and that H_2 desorption and adsorption is a legitimate chemical reaction. The distribution at 500 K is dramatically different: it is virtually uniform over the range 1.4 to 3.0 Å. The distribution at 300 K is intermediate in character and there is a significant probability that the center of mass of H_2 can be found as far as 2 Å from the surface. At these temperatures physisorption and desorption can no longer be regarded as rare events; therefore phenomenological kinetics can no longer consider them as elementary reactions. The classical and the quantum distribution of Z are not significantly different (Fig. 6); the latter is broader, presumably because of tunneling.

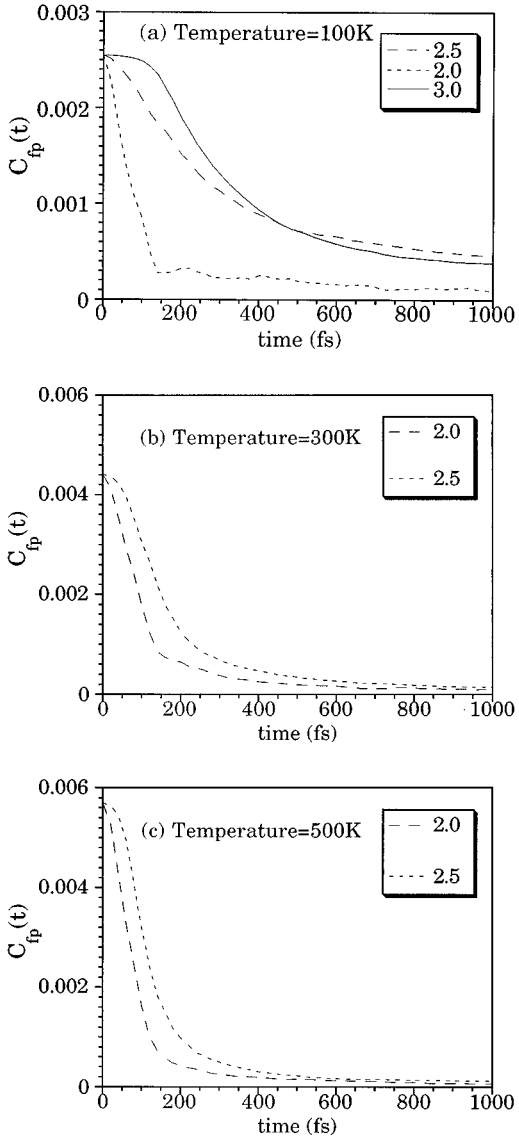

FIG. 7. Flux–position correlation functions $C_{fp}(t)$ for the physisorption and desorption processes as a function of time for different locations of the dividing surface $Z=Z_0$ at 100, 300, and 500 K. The Z_0 value (in Å) corresponding to each $C_{fp}(t)$ curve is shown on the graph.

The probability that physisorbed H_2 has a given bond length is weakly dependent on temperature and for this reason we show only the results for 100 K. In both the quantum and classical cases the probability of finding the system on the dividing surface separating physisorption from dissociation into chemisorbed H atoms is low. Therefore, the dissociation rate is well defined. The distribution function for r shows large quantum effects, presumably due to tunneling and zero point energy.

The probability that the axis of the physisorbed molecule makes an angle θ with the surface is centered at 90° and is broad. The ϕ distribution is nearly uniform. The distribution of X (or Y) is peaked around the origin of the unit cell (defined in Fig. 1). As expected the quantum distributions are somewhat more delocalized than the classical ones, especially along the X and Y coordinates.

The dependence of $C_{gp}(t)$ on time is shown in Fig. 7 for

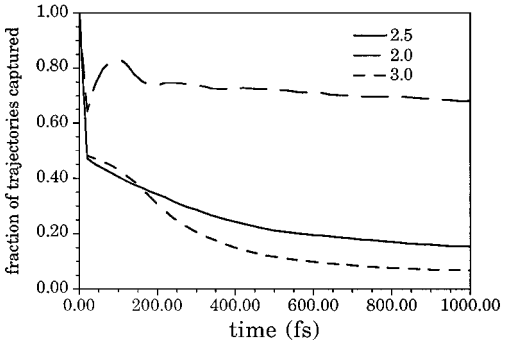

FIG. 8. Fraction of trajectories trapped in the physisorption minimum versus time for different positions of the dividing surface at a temperature of 100 K. The Z_0 value (in Å) corresponding to each curve is shown on the graph.

three different positions of the dividing surface ($Z_0=2.0$, 2.5, and 3.0 Å). At 100 K the correlation functions reach a plateau value in 1000 fs, for all values of Z_0. The qualitative behavior of the $Z_0=2.0$ Å curve differs from that of the other two. To understand this difference, it is helpful to consider the time dependence of $N_s(t)/N$ (Fig. 8) where N is the total number of trajectories run when computing $C_{gp}(t)$ and $N_s(t)$ is the number located, at time t, on the product side of the dividing surface. For $Z_0=2.0$ Å a large number of recrossings take place between 10 and 200 fs and then approximately 70% of the trajectories remain trapped on the products side of the dividing surface. For the other two curves, there is a sharp drop off followed by a few recrossings. This indicates the existence of a barrier between $Z=2.0$ Å and $Z=2.5$ Å. To understand the origin of this barrier we present (Fig. 9) the equilibrium classical probability distributions for the X and θ coordinates at different values of Z_0. The ϕ distribution was found to be nearly uniform and uninteresting, and the Y distribution is (by symmetry) identical to the X distribution. The probability distribution for the r coordinate is strongly peaked between $r=0.75$ Å and $r=0.8$ Å. From Fig. 9, it can be seen that at $Z_0=3.0$ Å, the initial configurations are distributed uniformly between $X=0$ and $0.5a$ where a is the unit cell parameter for the square 2D lattice formed by the surface atoms. However, as the dividing surface is moved closer to the solid (e.g., $Z_0=2.0$ Å), there is increased localization around the center of the unit cell. This means that the surface–molecule interaction energy goes up as the center of mass of the molecule moves away from the center of the unit cell (at fixed $Z=2.0$ Å). On the minimum energy reaction path (for physisorption) X and Y are at the center of the unit cell and the molecule is parallel to the surface. If $Z_0=2$ Å the energy of the molecule goes up when its geometry (i.e., X, Y, θ, ϕ) deviates from these values. If $Z_0=3$ Å there is practically no change.

The physisorption and desorption rates are given in Table II. Since the $C_{gp}(t)$ curves, particularly at 300 and 500 K, do not show a sharp onset of a plateau region, we also tabulate the time t at which we consider the flux–position correlation function to have reached a constant value. A more accurate calculation would include lattice motion and the resultant dissipation of energy by the solid surface should result in a better-defined plateau. The values of k_{gp} and k_{pg}

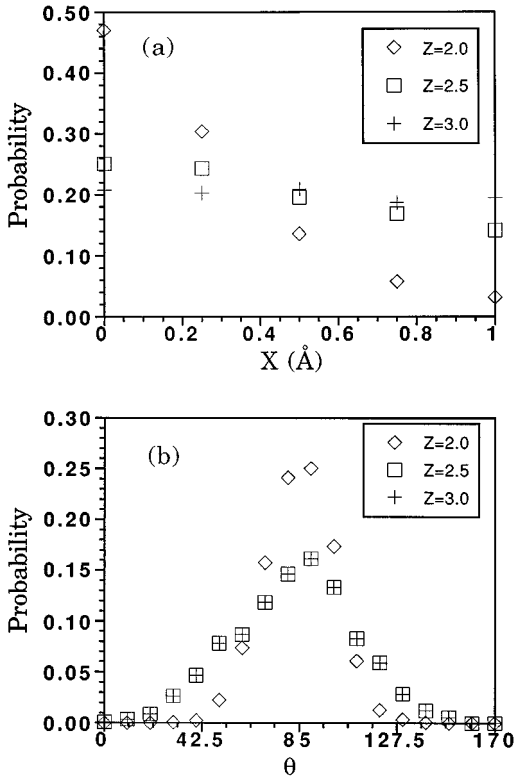

FIG. 9. Classical canonical probability distributions along the X (in Å) and θ (in degrees) coordinates at 100 K for different locations of the dividing surface $Z=Z_0$. The Z_0 value (in Å) corresponding to each distribution is shown on the graph.

at 300 and 500 K are listed even though at this temperature the rates no longer correspond to rare events; they give however an idea of the time scales involved.

In principle any reasonable choice of the dividing surface will give the same value for the rate constant. In practice a choice which passes through the point of maximum energy along the reaction path is better. The calculation of the rate constant makes use of the flux of the *reactive* trajectories going across the dividing surface. The trajectories are generated by a Monte Carlo procedure which gives the equilibrium velocities and positions of the H atoms when the molecule is on the dividing surface. If the dividing surface passes through the saddle point along the reaction path, most trajectories are reactive and the statistics in the Monte Carlo

TABLE II. The position Z_0 of the dividing surface for the adsorption of H_2 to form a physisorbed H_2 molecule, the plateau value $C_{gp}(t)$ of the flux–position correlation function at the time t when this value is reached, the physisorption rate constant k_{gp} and the desorption rate constant k_{pg}.

Temperature	Z_0(Å)	t (fs^{-1})	$C_{gp}(t)$	k_{gp} (Å fs^{-1})	k_{pg} (fs^{-1})
100 K	2.0	400	2.4 (−4)	3.0 (−4)	2.0 (−7)
	2.5	1000	4.9 (−4)	2.8 (−4)	1.8 (−7)
	3.0	1000	3.8 (−4)	3.1 (−4)	2.1 (−7)
300 K	2.0	400	2.5 (−4)	1.5 (−4)	8.5 (−5)
	2.5	500	3.5 (−4)	2.7 (−4)	1.1 (−4)
500 K	2.0	400	1.9 (−4)	1.3 (−4)	1.4 (−4)
	2.5	400	3.1 (−4)	2.7 (−4)	1.8 (−4)

TABLE III. Comparison of physisorption rate constants k_{gp} and the desorption rate constants k_{pg} (units of cm^{-3} sites^{-1} s^{-1}) calculated by using classical correlation function theory (this work) and variational transition state theory (Ref. 27).

	Correlation function		Variational TST	
Temperature	k_{gp}	k_{pg}	k_{gp}	k_{pg}
100 K	1.9 (−12)	1.9 (8)	2.5 (−11)	1.0 (10)
300 K	1.3 (−12)	9.7 (10)	7.7 (−12)	3.7 (12)
500 K	1.2 (−12)	1.6 (11)	3.1 (−12)	5.8 (12)

calculations are optimum. For other choices of the dividing surface, many trajectories do not react and the statistical properties of the reactive ones can be obtained only if one uses a very large number of MC moves. Unless this is done there are numerical discrepancies between the rates calculated for different positions of the dividing surface. Such differences are seen in the results presented in Table II.

We compare our results with those obtained by Truong, Hancock, and Truhlar[26] (THT) even though such a comparison is not very meaningful. THT have used canonical variational transition state theory (TST), and have included, in an approximate way, the role of lattice distortion and of the quantum effects. Such effects are absent in the present calculation. On the other hand, the transition state theory assumes that trajectories starting on the dividing surface never recross it. Our calculations of the flux–position correlation functions show that this assumption is erroneous. It is to some extent corrected by the variational procedure but it is still expected to provide an estimate of the rate constants that is too large. Thus compared to our calculations quantum effects will increase the rates and so will the use of TST. The effect of lattice distortion is harder to predict, but it is also likely to increase the rates.

For comparing our results with those in Ref. 26 we use the average of the rates obtained for the three values of Z_0. To convert the k_{gp} values in Table II to units of cm^{-3} site^{-1} s^{-1} we need to divide k_{gp} by the number of sites per unit area and convert from femtoseconds to seconds. The comparison is made in Table III. The two sets of physisorption rates are similar and decrease slowly with temperature. The desorption rates increase with temperature. The TST rates are an order of magnitude larger.

The dividing surface for chemisorption was set at $r=1.25$ Å. A consideration of the potential energy along the Z coordinate on the minimum energy surface shown in Fig. 3 at $r=1.25$ Å indicates that the potential is relatively flat in the range 0.5 Å$<Z<$1.0 Å and has two minima located at approximately $Z=0.6$ Å and $Z=0.9$ Å. The minimum at $Z=0.6$ Å ($X=Y=0$ Å and $\theta=0$) is slightly lower in energy than the minimum at $Z=0.9$ Å ($X=0$ Å, $Y=0.4$ Å, and $\theta=45$ deg). The molecular geometries in the two cases are different and the tilted geometry at $Z=0.9$ Å appears to be closer to the transition state geometry determined from the PES by Truong *et al.*[27] The population in the well centered at $Z=0.9$ Å increases significantly with temperature.

The flux–position correlation functions $C_{pc}(t)$ for this choice of dividing surface are shown in Fig. 10. All curves

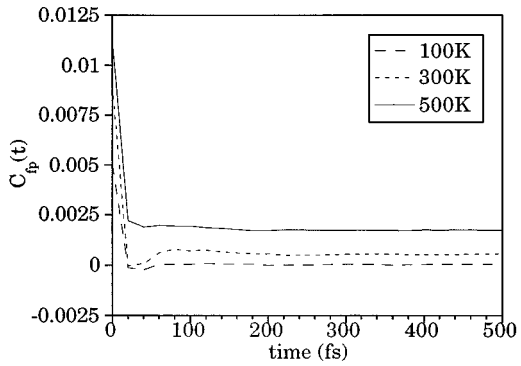

FIG. 10. Flux–position correlation functions $C_{fp}(t)$ for the chemisorption process as a function of time for dividing surface $r_0=1.25$ Å at 100, 300, and 500 K.

settle down to a well-defined plateau value within 100 fs. The plateau value of $C_{pc}(t)$ at 100 K is very small, indicating that there is massive recrossing of trajectories.

The calculated classical rate constants are presented along with the variational TST rates of Ref. 27 in Table IV. The values obtained with the classical correlation function theory are substantially lower than those of Truong and co-workers.[26] This difference is due to the approximations made by both theories. There is substantial recrossing which the TST theory does not take into account. On the other hand, we did not allow the lattice to relax as the hydrogen molecule moves along the reaction coordinate and have neglected the quantum effects. This large discrepancy suggests that it is worthwhile to attempt performing more accurate quantum correlation function calculations to assess the validity of the simplified (and highly efficient) theory presented by Truong *et al.*[26]

VII. SUMMARY

We have used here the classical correlation function theory to examine the rate of H_2 dissociation on the Ni(100) surface, for the Lee–DePristo model. In this model the reaction proceeds through a physisorbed intermediate at low temperatures and is direct at high ones. Phenomenological chemical kinetics has no difficulty describing these situations but offers no prescription for intermediate temperatures. Moreover, the kinetic equations for the two extreme cases do not go continuously into each other as the temperature passes through the intermediate range. The correlation function theory provides a set of equations having time-dependent rate constants. In the regime in which the phenomenological theory is valid, these time-dependent rate constants evolve

TABLE IV. The rate constants k_{pc} for the dissociative chemisorption calculated from classical correlation function theory (this work) and variational transition state theory (Ref. 27).

Temperature	Q_c	$C_{pc}(t)$	Correlation function k_{pc}	Variational TST k_{pc}
100 K	1.6 (−4)	5.0 (−5)	1.2 (4)	5.9 (7)
300 K	7.7 (−4)	5.5 (−4)	1.9 (8)	1.3 (11)
500 K	1.9 (−3)	1.7 (−3)	1.8 (9)	5.3 (11)

very rapidly to constant values which are equal to those provided by the phenomenology. The time in which the rate constants vary is so brief that it makes little difference to the observed kinetics, which is always studied at a long time scale. As the temperature is raised and the lifetime of a species becomes very short, the time-dependent rate constants involving that species will be different from zero only for a time interval comparable to the lifetime. As the lifetime becomes shorter, upon increasing the temperature, these rate constants contribute less and less to the kinetic process. These properties of the time-dependent rate constants are illustrated by simulations.

ACKNOWLEDGMENT

This work was supported by NSF Grant No. CHE 91129.

[1] M. Boudart and G. Djéga-Mariadassou, *Kinetics of Heterogenous Catalytic Reactions* (Princeton University, Princeton, 1984).
[2] R. P. H. Gasser, *An Introduction to Chemisorption and Catalysis by Metals* (Clarendon, Oxford, 1985).
[3] W. H. Weinberg, in *Kinetics of Interface Reactions*, edited by M. Grunze and H. J. Krenzer (Springer, Berlin, 1987).
[4] S. T. Ceyer, Annu. Rev. Phys. Chem. **39**, 479 (1988).
[5] A. E. DePristo and A. Kara, Adv. Chem. Phys. **77**, 163 (1990).
[6] R. B. Gerber, Chem. Rev. **87**, 29 (1987).
[7] C. Y. Lee and A. E. DePristo, J. Chem. Phys. **85**, 4161 (1986).
[8] A. Kara and A. E. DePristo, J. Chem. Phys. **88**, 5240 (1988).
[9] C. Y. Lee and A. E. DePristo, J. Chem. Phys. **87**, 1401 (1987).
[10] A. Kara and A. E. DePristo, J. Chem. Phys. **92**, 5653 (1990).
[11] P. E. M. Siegbahn, M. R. A. Blomberg, and C. W. Bauschlicher, Jr., J. Chem. Phys. **81**, 2103 (1984); T. H. Upton and W. A. Goddard III, Phys. Rev. Lett. **42**, 472 (1979); C. Umrigar and J. W. Wilkins, *ibid.* **54**, 1551 (1985); P. E. M. Siegbahn, M. R. A. Blomberg, I. Panas, and U. Wahlgren, Theor. Chim. Acta **75**, 143 (1988).
[12] T. Yamamoto, J. Chem. Phys. **33**, 281 (1960).
[13] (a) D. Chandler, J. Chem. Phys. **68**, 2959 (1978); (b) J. A. Montgomery, Jr., D. Chandler, and B. J. Berne, *ibid*. **70**, 4056 (1979).
[14] J. L. Skinner and P. J. Wolnyes, J. Chem. Phys. **69**, 2143 (1978); **72**, 4913 (1980).
[15] A. F. Voter and J. D. Doll, J. Chem. Phys. **82**, 80 (1985).
[16] W. H. Miller, S. D. Schwartz, and J. W. Tromp, J. Chem. Phys. **79**, 4889 (1983).
[17] G. Wahnstrom and H. Metiu, J. Phys. Chem. **92**, 3240 (1988).
[18] G. Wahnstrom, B. Carmeli, and H. Metiu, J. Chem. Phys. **88**, 2478 (1988).
[19] Z. Zhang, K. Haug, and H. Metiu, J. Chem. Phys. **93**, 3614 (1990).
[20] K. Haug, G. Wahnstrom, and H. Metiu, J. Chem. Phys. **92**, 2083 (1990); K. Haug and H. Metiu, *ibid*. **94**, 3251 (1991).
[21] G. A. Voth, D. Chandler, and W. H. Miller, J. Phys. Chem. **93**, 7010 (1989).
[22] B. J. Berne, in *Multiple Time Scales*, edited by J. U. Brackbill and B. I. Cohen (Academic, Orlando, 1985).
[23] J. T. Hynes, in *Theory of Chemical Reactions*, edited by M. Baer (Chemical Rubber, Boca Raton, 1985).
[24] G. Wahnstrom and H. Metiu, Chem. Phys. Lett. **145**, 44 (1988).
[25] G. Wahnstrom, J. Chem. Phys. **89**, 6996 (1988).
[26] T. N. Truong, G. Hancock, and D. G. Truhlar, Surf. Sci. **214**, 523 (1989).
[27] T. N. Truong, D. G. Truhlar, and B. C. Garrett, J. Phys. Chem. **93**, 8227 (1989).
[28] S. W. Lovesey, *Condensed Matter Physics: Dynamic Correlations* (Benjamin/Cummings, New York, 1986).
[29] M. P. Allen and D. J. Tildesley, *Computer Simulations of Liquids* (Clarendon, Oxford, 1991).
[30] D. W. Heermann, *Computer Simulation Methods in Theoretical Physics* (Springer, Berlin, 1990).
[31] Z. Zhang and H. Metiu, J. Chem. Phys. **93**, 2087 (1990).
[32] C. Y. Lee and A. E. DePristo, J. Chem. Phys. **84**, 485 (1986).
[33] C. H. Bennett, J. Comput. Phys. **22**, 245 (1976).
[34] J. D. Doll, D. L. Freeman, and T. L. Beck, Adv. Chem. Phys. **78**, 61 (1990).